

**Comparative Study of dG Affinity vs. DNA Methylation Modulating
Properties of Side Chain Derivatives of Procainamide: Insight Into Its DNA
Hypomethylating Effect**

R. L. Gawade,^a D. K. Chakravarty,^b J. Debgupta,^c E. Sangtani,^a S. Narwade,^b R. G. Gonnade,^a
V. G. Puranik,^{a*} and D. D. Deobagkar^{b*}

Electronic Supplementary Information

Entry	Contents	Page
1.	General scheme of synthesis of compounds 1-6	S4
2.	Figure S1. General scheme of synthesis	S5
3.	Preparation of 4-amino-N-phenethylbenzamide (1)	S6
4.	Figure S2. ¹ H NMR of 4-amino-N-phenethylbenzamide.	S6
5.	Figure S3. HR-MS of 4-amino-N-phenethylbenzamide.	S7
6.	Preparation of 4-amino-N-(2-(pyrrolidin-1-yl)ethyl)benzamide (2)	S8
7.	Figure S4. ¹ H NMR of 4-amino-N-(2-(pyrrolidin-1-yl)ethyl)benzamide	S8
8.	Figure S5. HR-MS study 4-amino-N-(2-(pyrrolidin-1-yl) ethyl) benzamide.	S9
9.	Preparation of 4-amino-N-(2-(dimethylamino)ethyl)benzamide (3)	S10
10.	Figure S6. ¹ H NMR of 4-amino-N-(2-(dimethylamino) ethyl) benzamide	S10
11.	Figure S7. HR-MS study of 4-amino-N-(2-(dimethylamino) ethyl) benzamide	S11
12.	Preparation of 4-amino-N-(2-morpholinoethyl)benzamide (4)	S12
13.	Figure S8. ¹ H NMR of 4-amino-N-(2-morpholinoethyl)benzamide	S12
14.	Figure S9. HR-MS of 4-amino-N-(2-morpholinoethyl)benzamide	S13
15.	Preparation of 4-amino-N-(2-(piperidin-1-yl)ethyl)benzamide (5)	S14
16.	Figure S10. ¹ H NMR of 4-amino-N-(2-(piperidin-1-yl) ethyl) benzamide	S14
17.	Figure S11. HR-MS of 4-amino-N-(2-(piperidin-1-yl)ethyl)benzamide	S15
18.	Preparation of 4-amino-N-(2-(pyridin-2-yl)ethyl)benzamide (6)	S16
19.	Figure S12. ¹ H NMR of 4-amino-N-(2-(pyridin-2-yl)ethyl)benzamide.	S16
20.	Figure S13. HR-MS of 4-amino-N-(2-(pyridin-2-yl) ethyl) benzamide.	S17
21.	Figure S14. HPLC purity profile of compound 1 (Phenyl)	S18
22.	Figure S15. HPLC purity profile of compound 2 (Pyrrolidine)	S19
23.	Figure S16. HPLC purity profile of compound 3 (Dimethyl)	S20
24.	Figure S17. HPLC purity profile of compound 4 (Morpholine)	S21
25.	Figure S18. HPLC purity profile of compound 5 (Piperidine)	S22
26.	Figure S19. HPLC purity profile of compound 6 (Pyridine)	S23
27.	X-ray Crystallography	S24
28.	Table S1: Crystallographic data table of compounds 1-6	S25
29.	Figure S20. ORTEP diagrams of compounds (a) 1 (b) 2 (c) 3 (d) 4 (e) 5 and (f) 6	S27

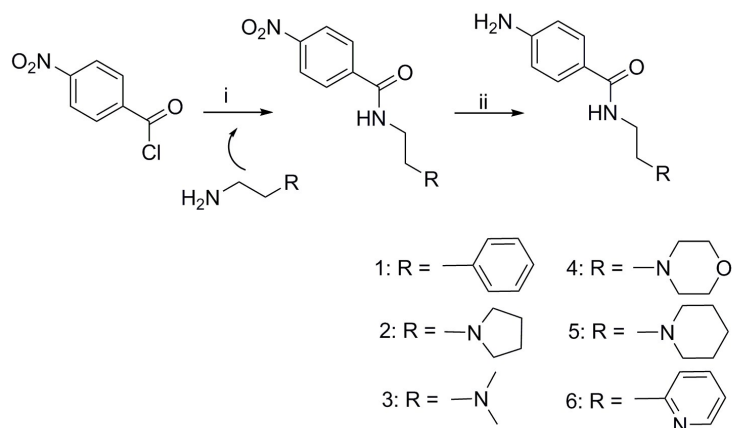
30.	Differential Pulse Voltametry	S28
31.	Figure S21. Differential pulse voltammogram of phenyl drug alone under identical condition used for the study of drug-dG interactions, DPV for only buffer (blank) is also shown for comparison; appearance of peak in case of phenyl drug suggests oxidation of drug molecule	S28
32.	Docking Study	S29
33.	CSD survey	S30
34.	Figure S22. (a) Molecular structure of query (b) XY plot of X-torsion range and Y- number of hits in %	S30
35.	Table S2. Number of hits , torsion angle range in %	S30
36.	Figure S23. Overlay of active conformers compounds 1-6 and Procainamide chosen after torsional filtering.	S31
37.	Table S3. Torsion angle table τ_1 of ligand conformations from selected docked poses.	S31
38.	Figure S24. $\pi \cdots \pi$ stacking geometry of compound 6 (pyridine) with dG base at the target site (extracted from docked pose) displaying Cg \cdots Cg distance (centroid to centroid distance between aromatic rings) and dihedral angle α between the aromatic rings.	S31
39.	Cytotoxicity Assay	S32
40.	Figure S25. Cell viability study after 24h time point for compounds 1-6 and Procainamide and concentration ranging from 100-500 μ M. (X: conc. of compounds and Y: Cell viability in %)	S33
41.	Figure S26. Cell viability study after 48h time point for compounds 1-6 and Procainamide and concentration ranging from 100-500 μ M. (X: conc. of compounds and Y: Cell viability in %)	S34
42.	Figure S27. Cell viability study after 72h time point for compounds 1-6 and Procainamide and concentration ranging from 100 μ M -500 μ M. (X: conc. of compounds and Y: Cell viability in %)	S35
43.	Global Methylation Quantification Assay	S36
44.	DNMT-1 inhibition assay	S37
45.	References	S38

General scheme of synthesis of compounds 1-6

The compounds **1-6** were synthesized as per the reported procedure. To the stirring solution of primary amines (21.56 mmol, 2 equi.) in dry DCM, dry Et₃N (3.76 ml, 26.95 mmol, 2.5 equi.) was added drop wise followed by slow addition of 4-nitrobenzoyl chloride (2g, 10.78 mmol) in dry DCM (20 ml) at 0°C. The reaction mixture was allowed to reach room temperature and was further stirred for 8 h. The solvent was evaporated under vacuum and EtOAc solvent was added to the crude solid reaction product. The mixture was then sequentially washed twice with saturated solution of NaHCO₃ and once with brine. The organic layer was dried over anhydrous Na₂SO₄ and evaporated under vacuum to obtain crude nitro intermediate product. 4-nitro carboxamide intermediate was used without purification for reduction step (ii).

Nitro to amine reduction was carried out in the presence of catalytic amount (10%) of Pd/C, H₂ (60 mbar) in EtOH solvent at room temperature. After 8-9 h of reaction time, completion of reaction was monitored by thin layer chromatography (EtOAc:MeOH; 95:5) solvent system and ninhydrin reagent (pink colouration for amine spot was observant). The crude reaction mixture was filtered through celite bed to remove Pd catalyst and solvent was evaporated under vacuum to yield crude solid compound. Purification was carried out using column chromatography (20 % EtOAc:Petroleum Ether to 3% MeOH: EtOAc solvent system) to yield compound **1-6**. Purified products were further crystallized from DCM/Petroleum Ether solvent system to obtain single crystals for crystal structure analysis and biological studies.

NMR spectra were recorded on AC 200MHz Bruker NMR spectrometer and HR-MS spectra were obtained from Thermoscientific Q Exactive instrument.



Reagents and condition: (i) DCM, Et₃N, 2-Phenethylamine for 1, 1-(2-Aminoethyl)pyrrolidine for 2, N,N-Dimethylethylenediamine for 3, 4-(2-Aminoethyl)morpholine for 4, 1-(2-Aminoethyl)piperidine for 5, 2-(2-Pyridyl)ethylamine for 6, RT, 8h, (ii) EtOH, Pd/C, H₂, 60 mbar, RT, 8h.

Figure S1. General scheme of synthesis

Experimental Synthesis:

4-amino-N-phenethylbenzamide (1) was prepared as above (general scheme of synthesis) using phenethyl amine (2.72 ml, 21.56 mmol, 2 equ.) to yield compound **1**. ^1H NMR (200MHz, CDCl_3) δ = 7.61 - 7.47 (m, 2 H), 7.39 - 7.27 (m, 2 H), 7.27 - 7.18 (m, 3 H), 6.75 - 6.55 (m, 2 H), 5.99 (br. s., 1 H), 3.95 (br. s., 2 H), 3.70 (q, J = 6.8 Hz, 3 H), 2.92 (t, J = 6.8 Hz, 2 H); HR-MS: ($\text{C}_{15}\text{H}_{16}\text{N}_2\text{O}$) 241.1335 ($\text{M}+\text{H}$) $^+$, 263.1154 ($\text{M}+\text{Na}$) $^+$.

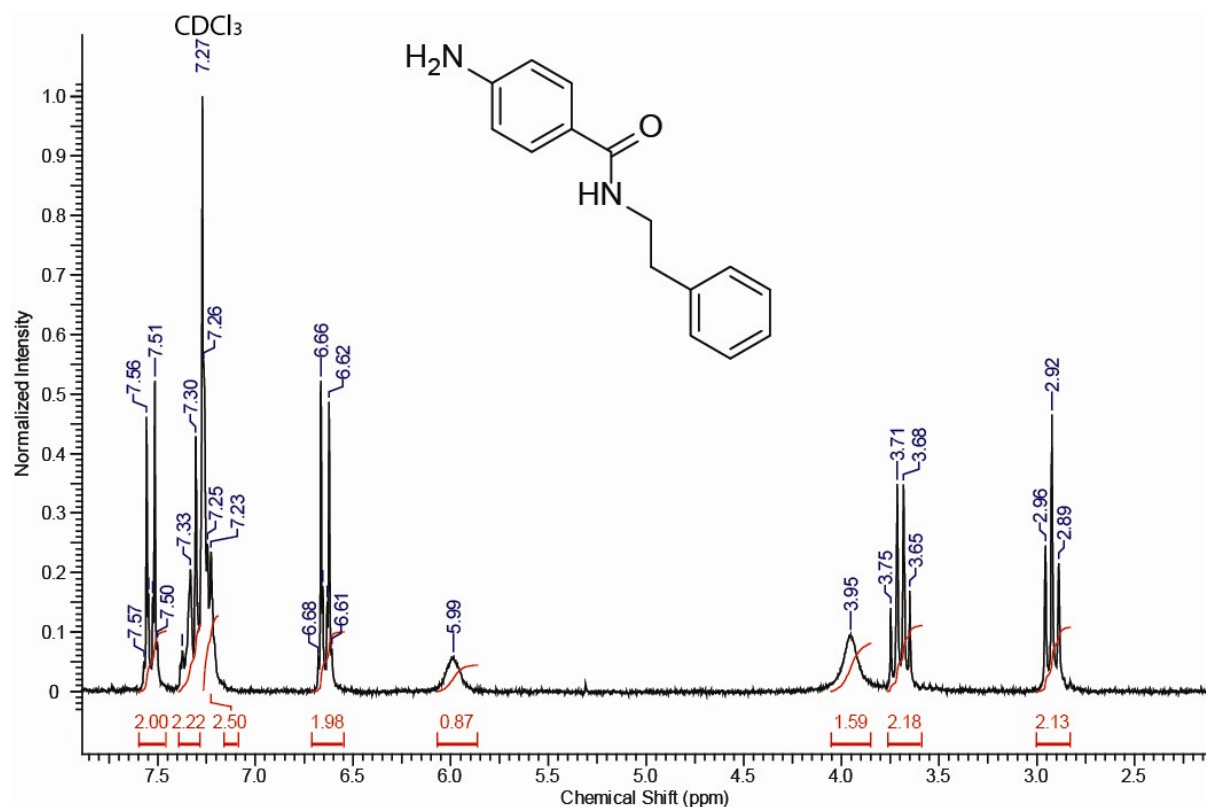


Figure S2. ^1H NMR of 4-amino-N-phenethylbenzamide.

PHE_RJ #864 RT: 3.85 AV: 1 NL: 5.54E8
T: FTMS + p ESI Full ms [60.00-900.00]

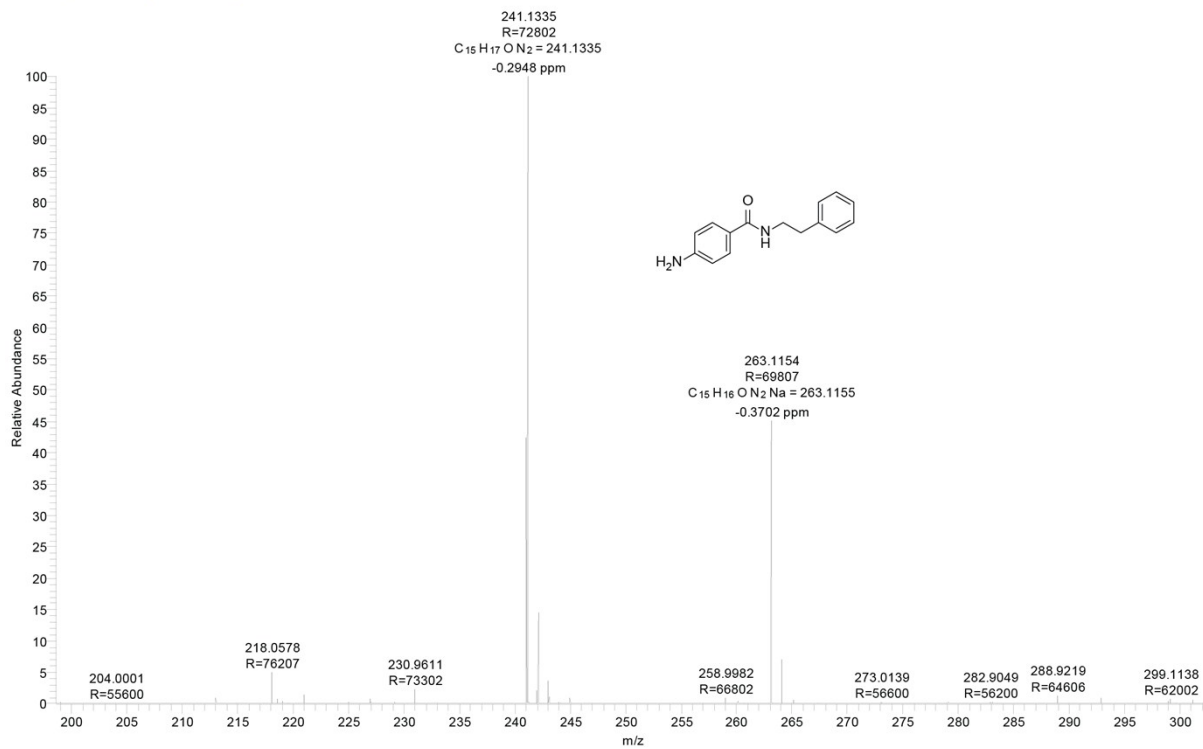


Figure S3. HR-MS of 4-amino-N-phenethylbenzamide.

4-amino-N-(2-(pyrrolidin-1-yl)ethyl)benzamide (2) was prepared as above using 2-pyrrolidinoethylamine, (2.73 ml, 21.56 mmol, 2 equi.) to yield compound **2**. ^1H NMR (200MHz, CDCl_3) $\delta = 7.63$ (d, $J = 8.6$ Hz, 2 H), 6.67 (m, 3 H), 3.95 (br. s., 2 H), 3.53 (q, $J = 5.3$ Hz, 2 H), 2.69 (m, 2 H), 2.56 (m, 4 H), 1.79 (m, 4 H); HR-MS: ($\text{C}_{13}\text{H}_{19}\text{N}_3\text{O}$) 234.1601 ($\text{M}+\text{H}$) $^+$.

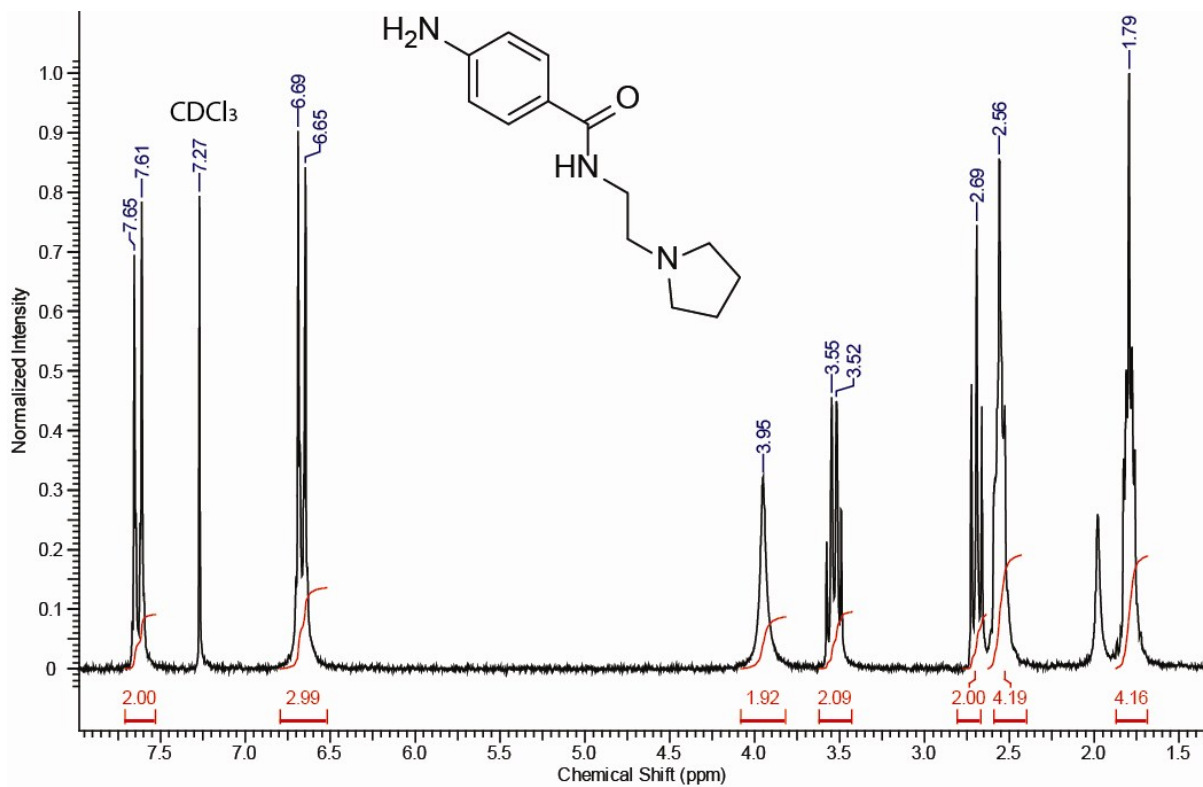


Figure S4. ^1H NMR of 4-amino-N-(2-(pyrrolidin-1-yl)ethyl)benzamide

PYRR_RJ#477 RT: 2.12 AV: 1 NL: 1.12E9
T: FTMS + p ESI Full ms [60.00-900.00]

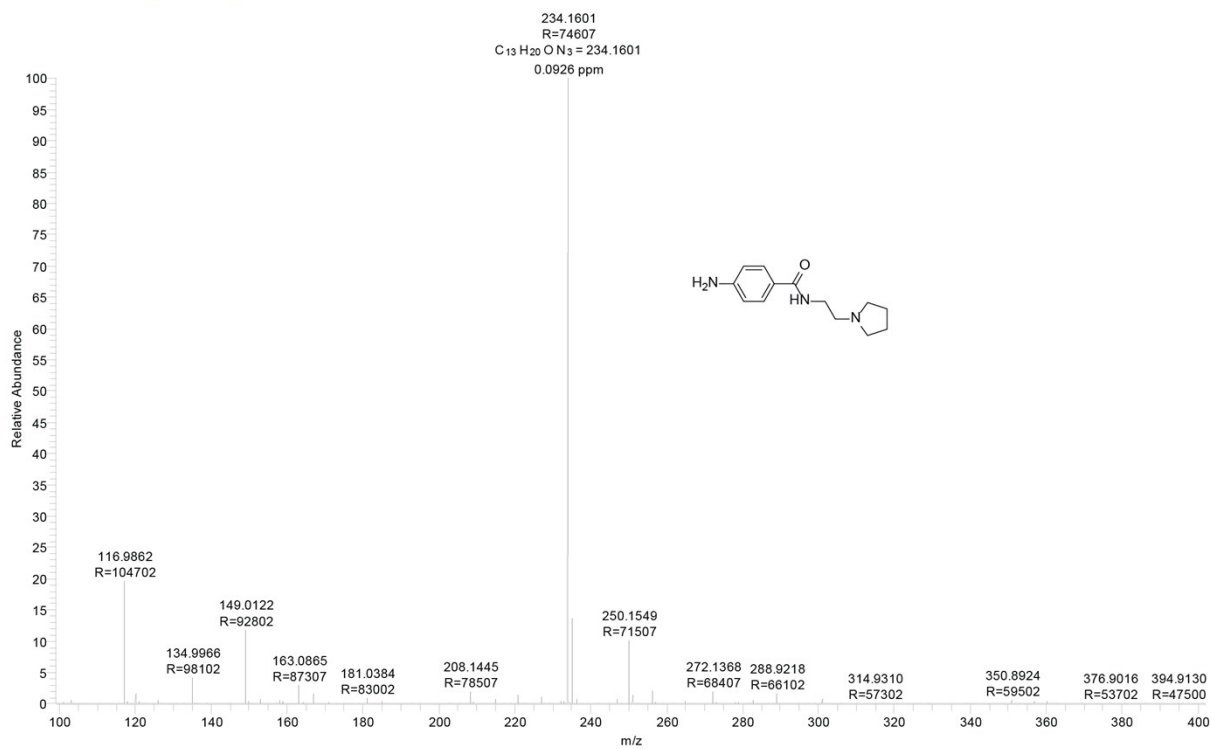


Figure S5. HR-MS study 4-amino-N-(2-(pyrrolidin-1-yl)ethyl)benzamide

4-amino-N-(2-(dimethylamino)ethyl)benzamide (3) was prepared as above using 2-(Dimethylamino)ethylamine, (2.36 ml, 21.56 mmol, 2 equ.) to yield compound **3**. $^1\text{H NMR}$ (200MHz, CDCl_3) δ = 7.70 - 7.56 (m, 2 H), 6.76 - 6.57 (m, 3 H), 3.96 (br. s., 2 H), 3.58 - 3.42 (m, 2 H), 2.51 (t, J = 5.9 Hz, 2 H), 2.31 - 2.20 (m, 6 H). HR-MS: ($\text{C}_{11}\text{H}_{17}\text{N}_3\text{O}$) 208.1444 ($\text{M}+\text{H}$) $^+$, 230.1262 ($\text{M}+\text{Na}$) $^+$

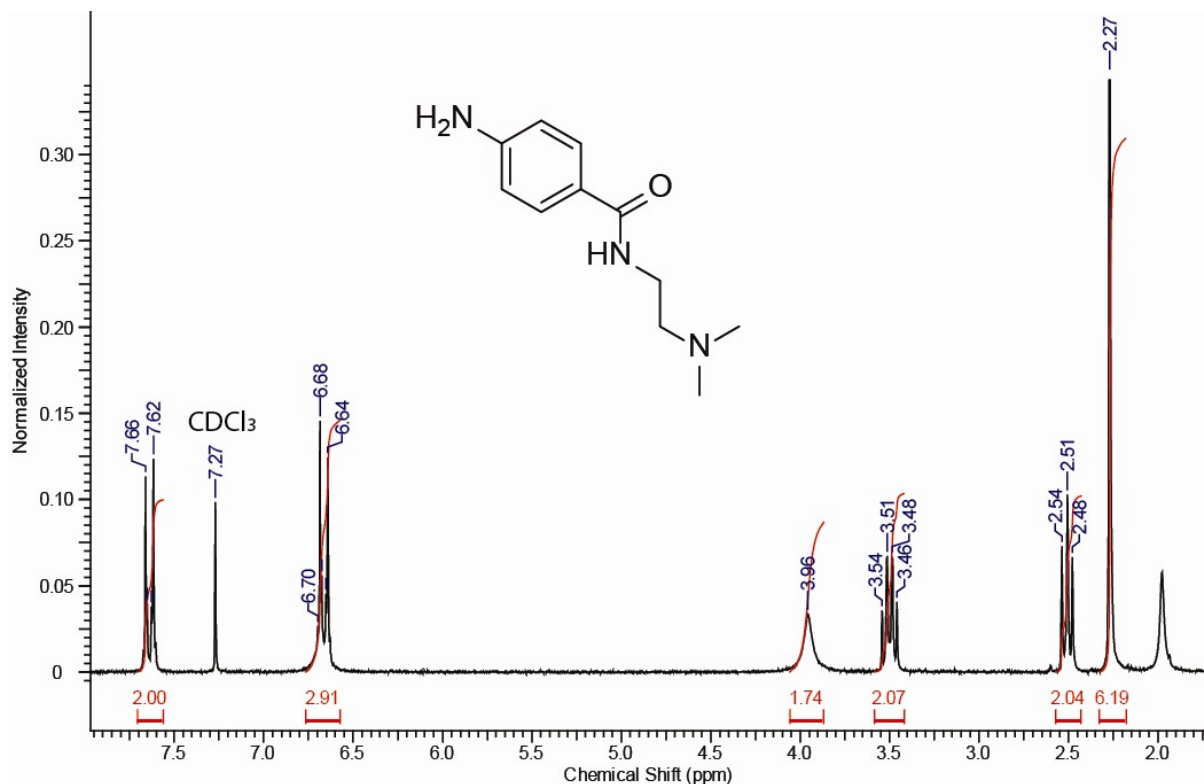


Figure S6. $^1\text{H NMR}$ of 4-amino-N-(2-(dimethylamino)ethyl)benzamide

DIM_RJ #472 RT: 2.10 AV: 1 NL: 1.18E9
T: FTMS + p ESI Full ms [60.00-900.00]

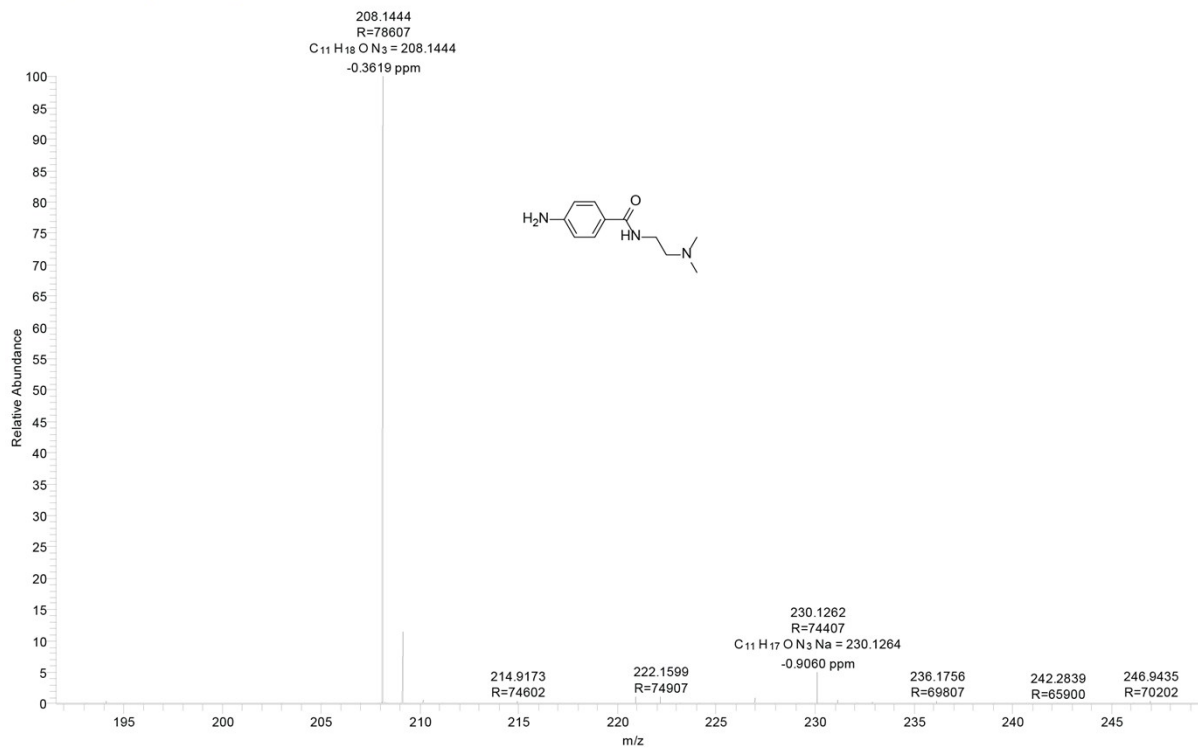


Figure S7. HR-MS study of 4-amino-N-(2-(dimethylamino)ethyl)benzamide

4-amino-N-(2-morpholinoethyl)benzamide (4) was prepared as above using 2-morpholinoethylamine, (2.83 ml, 21.56 mmol, 2 equi.) to yield compound 4. ^1H NMR (200MHz, CDCl_3) δ = 7.69 - 7.52 (m, 2 H), 6.73 - 6.64 (m, 2 H), 6.61 (br. s., 1 H), 3.97 (br. s., 2 H), 3.83 - 3.63 (m, 4 H), 3.60 - 3.41 (m, 2 H), 2.59 (t, J = 6.1 Hz, 2 H), 2.55 - 2.42 (m, 4 H); HR-MS: ($\text{C}_{13}\text{H}_{19}\text{N}_3\text{O}_2$) 250.1550 ($\text{M}+\text{H}$) $^+$.

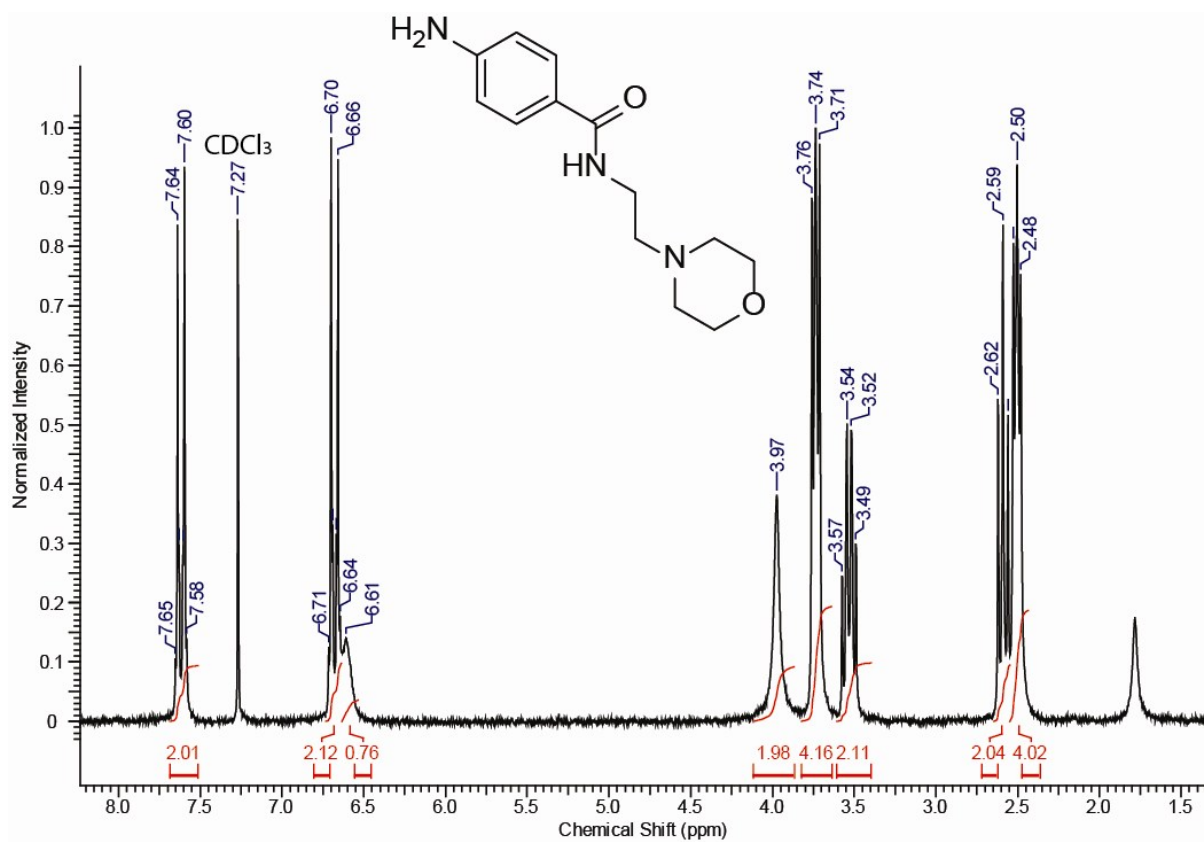


Figure S8. ^1H NMR of 4-amino-N-(2-morpholinoethyl)benzamide

MOR_RJ #488 RT: 2.17 AV: 1 NL: 1.08E9
T: FTMS + p ESI Full ms [60.00-900.00]

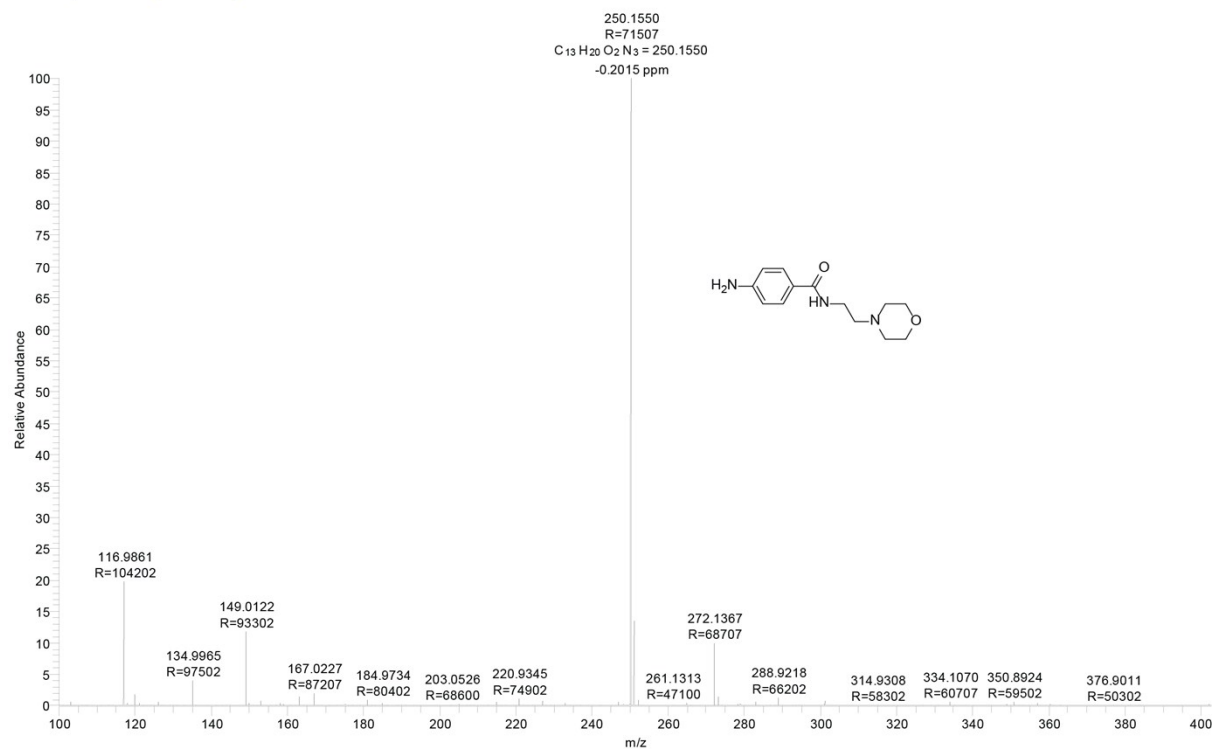


Figure S9. HR-MS of 4-amino-N-(2-morpholinoethyl)benzamide

4-amino-N-(2-(piperidin-1-yl)ethyl)benzamide (5) was prepared as above using 2-Piperidinoethylamine, (3.07 ml, 21.56 mmol, 2 equi.) to yield compound **5**. $^1\text{H NMR}$ (200MHz, CDCl_3) δ = 7.70 - 7.53 (m, 2 H), 6.81 (br. s., 1 H), 6.72 - 6.55 (m, 2 H), 3.96 (br. s., 2 H), 3.59 - 3.42 (m, 2 H), 2.55 (t, J = 6.1 Hz, 2 H), 2.43 (d, J = 5.2 Hz, 4 H), 1.69 - 1.53 (m, 4 H), 1.53 - 1.34 (m, 2 H); HR-MS: ($\text{C}_{14}\text{H}_{21}\text{N}_3\text{O}$) 248.1756 ($\text{M}+\text{H}$) $^+$.

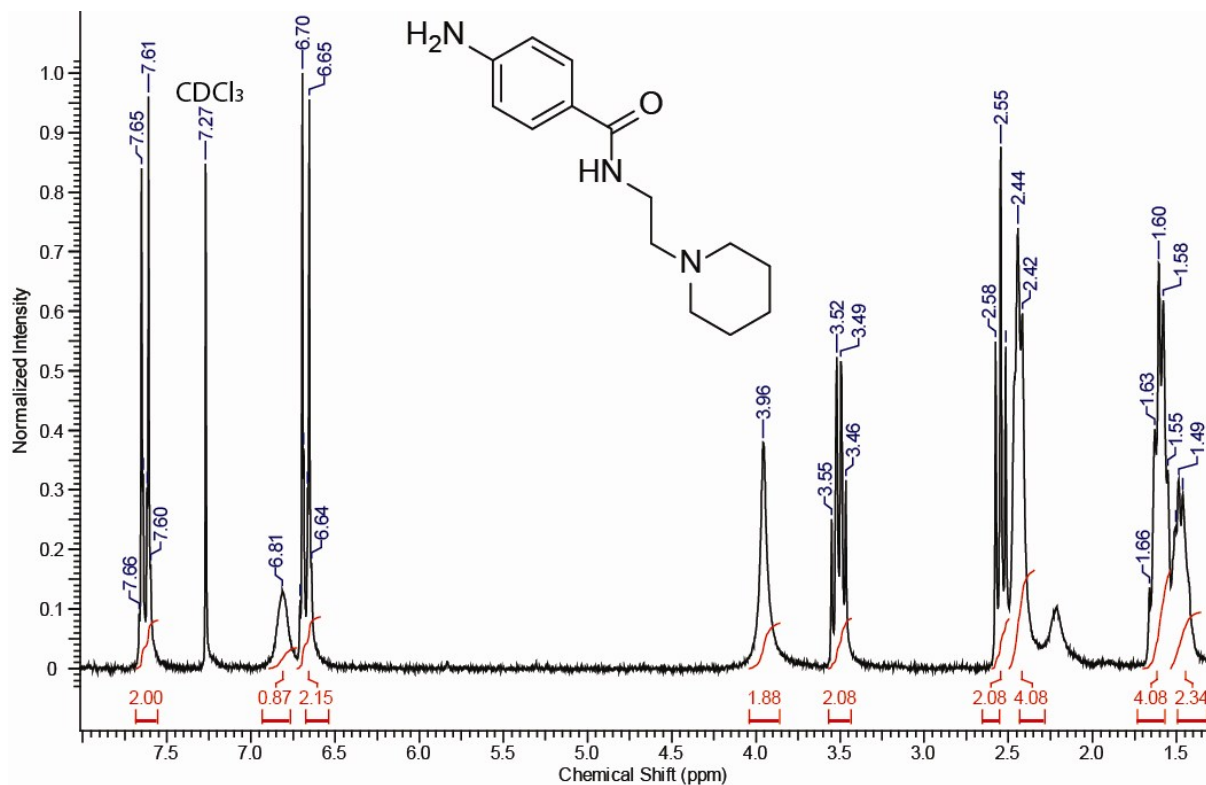


Figure S10. $^1\text{H NMR}$ of 4-amino-N-(2-(piperidin-1-yl)ethyl)benzamide

PIP_RJ #462 RT: 2.06 AV: 1 NL: 1.27E9
T: FTMS + p ESI Full ms [60.00-900.00]

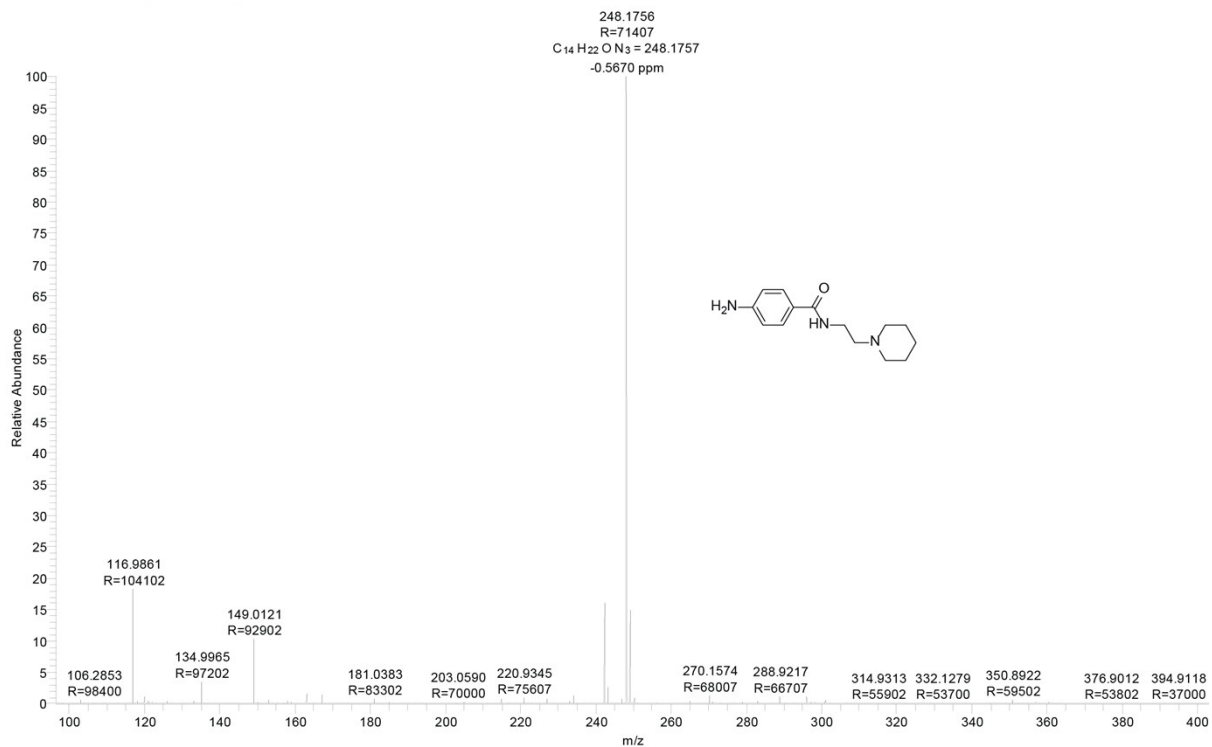


Figure S11. HR-MS of 4-amino-N-(2-(piperidin-1-yl)ethyl)benzamide

4-amino-N-(2-(pyridin-2-yl)ethyl)benzamide (6) was prepared as above using 2-(2-Pyridyl)ethylamine, (2.58 ml, 21.56 mmol, 2 equ.) to yield compound **6**. $^1\text{H NMR}$ (200MHz, Acetonitrile- d_3) δ = 8.31 - 8.30 (m, 1 H), 7.51 - 7.37 (m, 1 H), 7.29 (d, J = 8.3 Hz, 2 H), 7.07 - 6.78 (m, 3 H), 6.40 (d, J = 8.5 Hz, 2 H), 4.31 (br. s., 2 H), 3.44 (q, J = 6.6 Hz, 2 H), 2.78 (t, J = 6.9 Hz, 2 H); HR-MS: ($\text{C}_{14}\text{H}_{15}\text{N}_3\text{O}$) 242.1288 ($\text{M}+\text{H}$) $^+$.

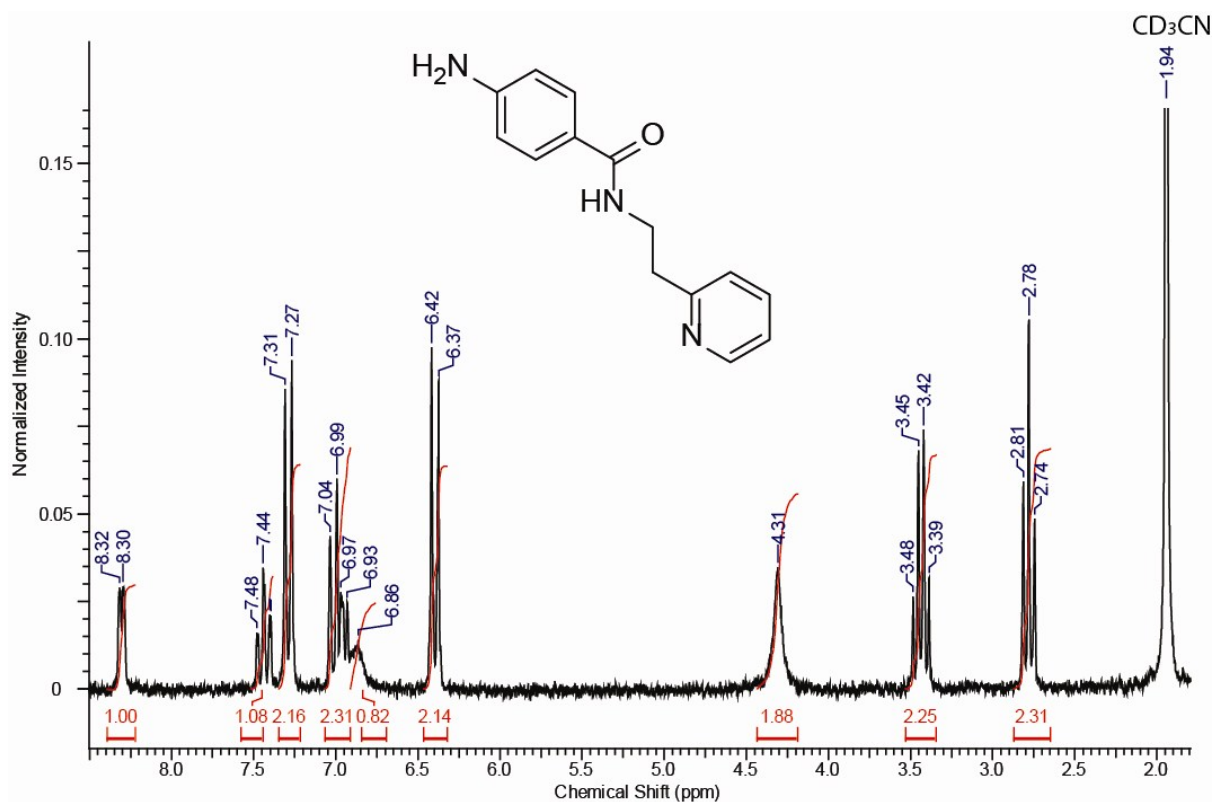


Figure S12. $^1\text{H NMR}$ of 4-amino-N-(2-(pyridin-2-yl)ethyl)benzamide.

PYRI_RJ #728 RT: 3.24 AV: 1 NL: 7.04E8
T: FTMS + p ESI Full ms [60.00-900.00]

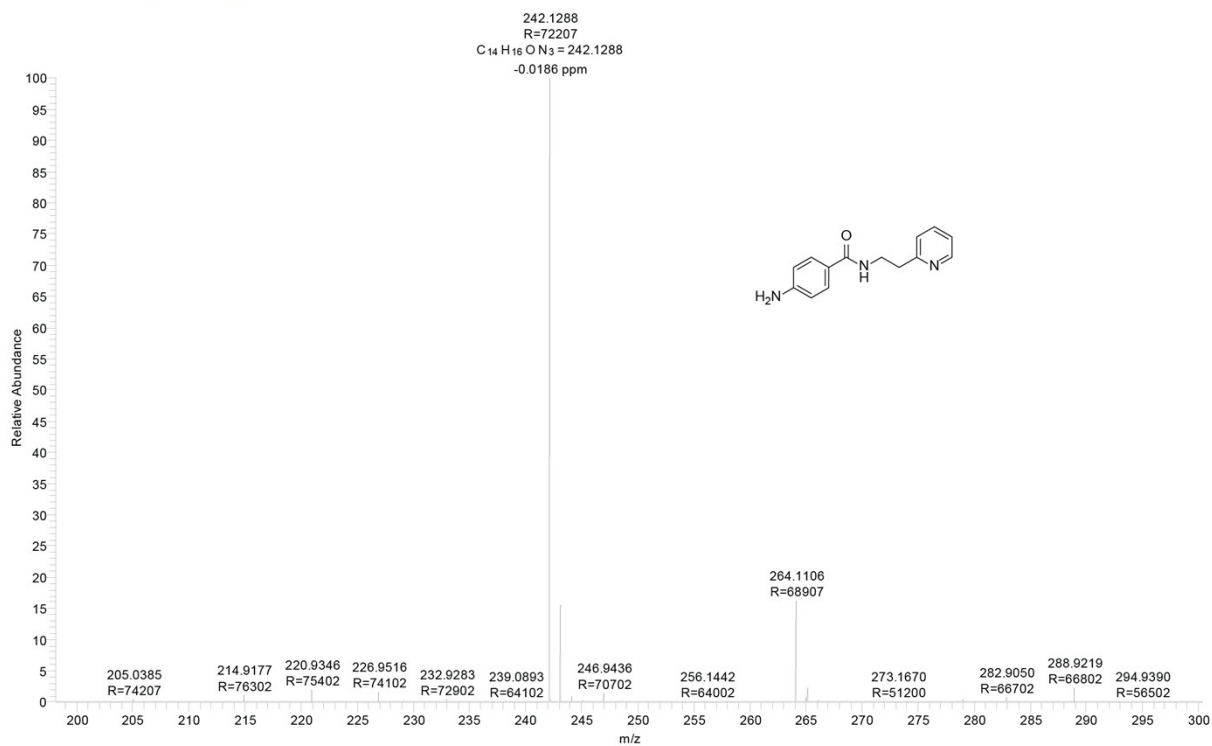
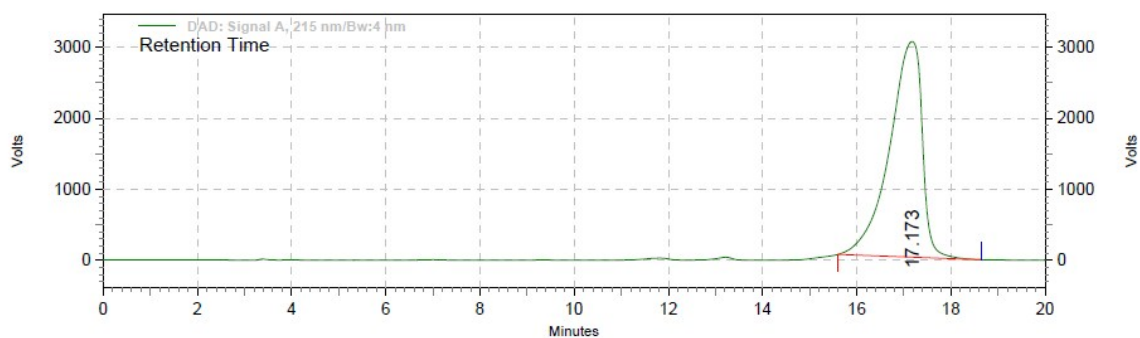


Figure S13. HR-MS NMR of 4-amino-N-(2-(pyridin-2-yl)ethyl)benzamide.

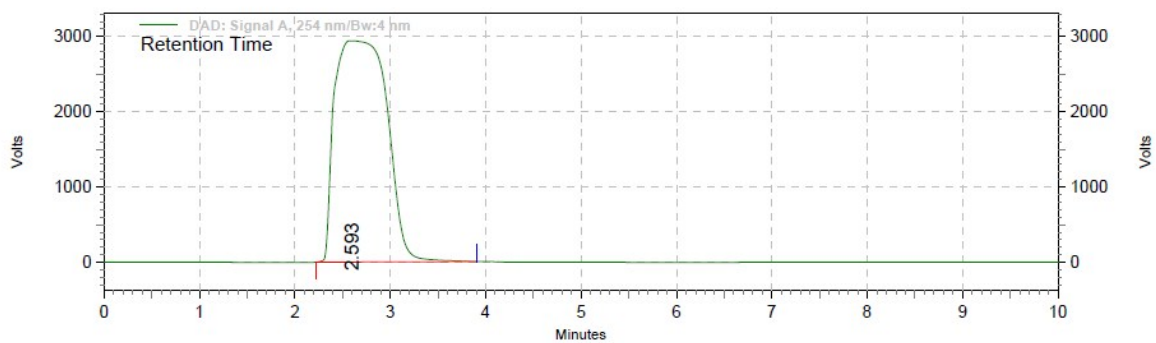


DAD: Signal A,
215 nm/Bw:4 nm
Results

Retention Time	Area	Area %	Height	Height %
17.173	306667676	100.00	6366379	100.00
Totals	306667676	100.00	6366379	100.00

Column: C18
Flow rate: 1ml/min
Solvent system: 50% MEOH 50% H2O

Figure S14. HPLC % purity profile of Compound 1 (Phenyl)

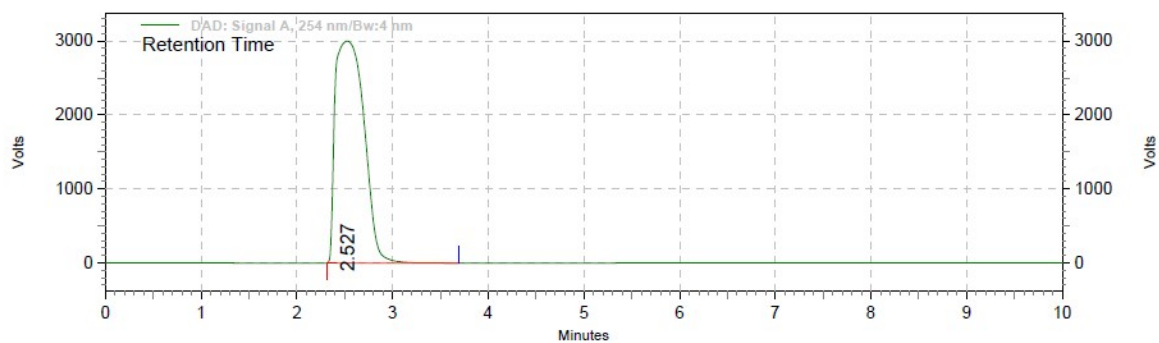


**DAD: Signal A,
254 nm/Bw:4 nm
Results**

Retention Time	Area	Area %	Height	Height %
2.593	235132622	100.00	6171088	100.00
Totals	235132622	100.00	6171088	100.00

Column: C18
Flow rate: 1ml/min
Solvent system: 40% MEOH 60% H2O

Figure S15. HPLC % purity profile of Compound 2 (Pyrrolidine)

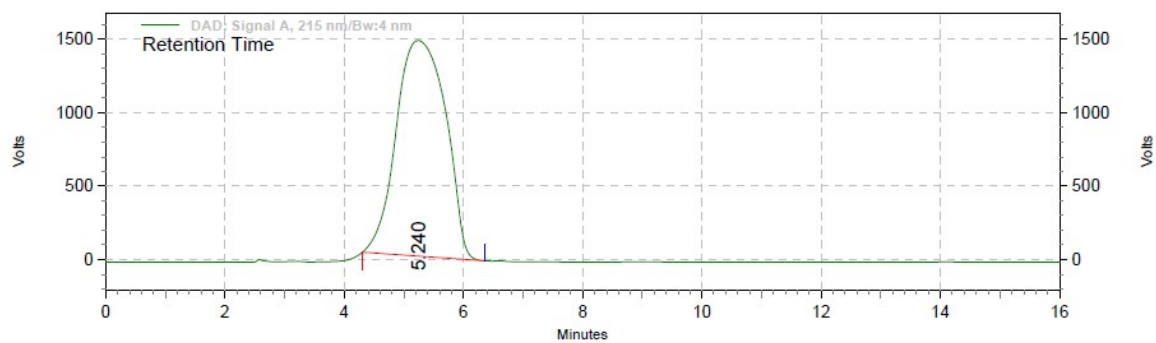


**DAD: Signal A,
254 nm/Bw:4 nm
Results**

Retention Time	Area	Area %	Height	Height %
2.527	132152744	100.00	6293410	100.00
Totals		132152744	6293410	100.00

Column: C18
Flow rate: 1ml/min
Solvent system: 40% MEOH 60% H2O

Figure S16. HPLC % purity profile of Compound 3 (Dimethyl)

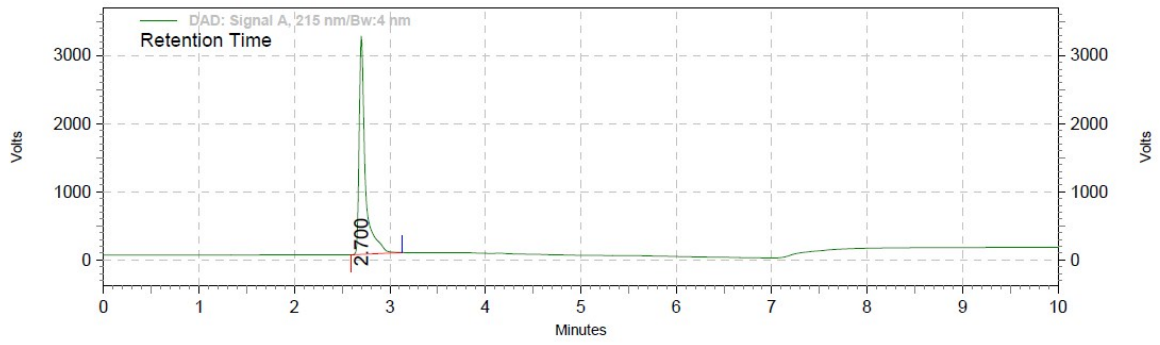


**DAD: Signal A,
215 nm/Bw:4 nm
Results**

Retention Time	Area	Area %	Height	Height %
5.240	178026317	100.00	3078417	100.00
Totals		178026317	3078417	100.00

Column : C18
Flow Rate- 1.0 ml/min
Eluent: 30%MEOH 70%H2O

Figure S17. HPLC % purity profile of Compound 4 (Morpholine)

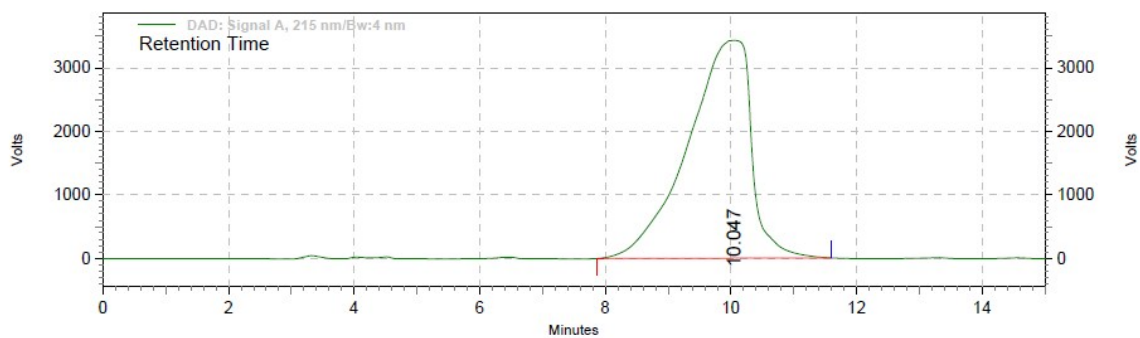


**DAD: Signal A,
215 nm/Bw:4 nm
Results**

Retention Time	Area	Area %	Height	Height %
2.700	30231970	100.00	6719091	100.00
Totals		30231970	6719091	100.00

Column: C18
Flow rate: 1ml/min
Solvent system: 40% MEOH 60% H2O

Figure S18. HPLC % purity profile of Compound 5 (Piperidine)



**DAD: Signal A,
215 nm/Bw:4 nm
Results**

Retention Time	Area	Area %	Height	Height %
10.047	505561942	100.00	7196492	100.00
Totals	505561942	100.00	7196492	100.00

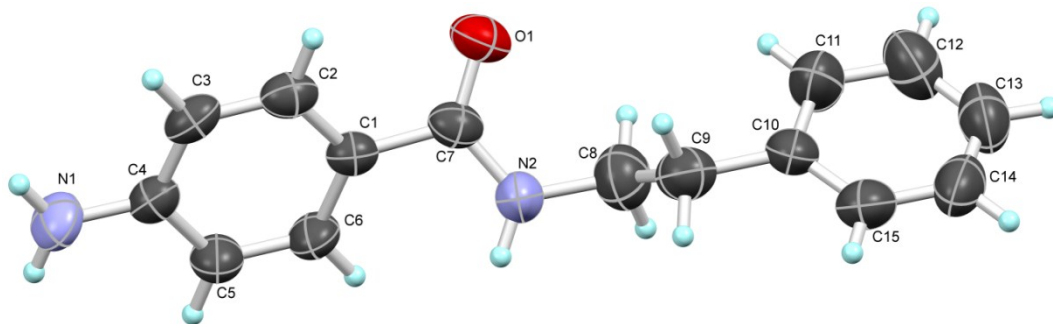
Column: C18
Flow rate: 1ml/min
Solvent system: 40% MEOH 60% H2O

Figure S19. HPLC % purity profile of Compound 6 (Pyridine)

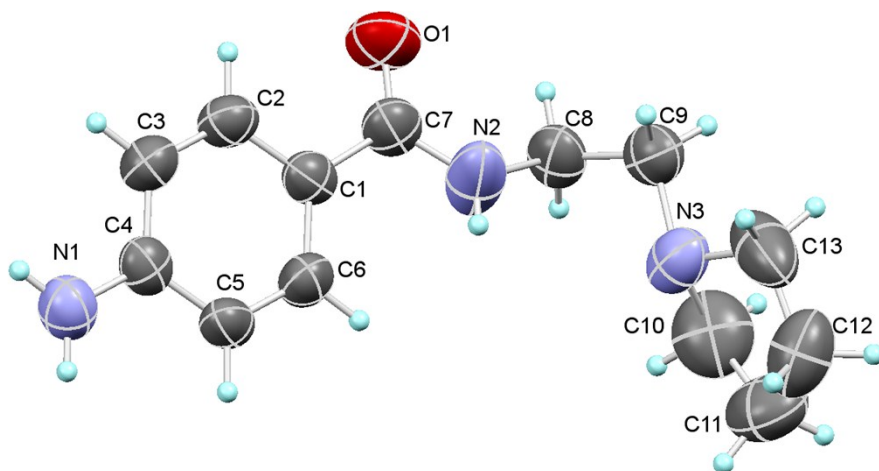
X-ray Crystallography: Single crystal structure of all compounds **1-6** were determined by measuring X-ray intensity data on a Bruker SMART APEX II single crystal X-ray CCD diffractometer having graphite-monochromatised Mo-K α ($\lambda = 0.71073$ Å) radiation. The X-ray generator was operated at 50 kV and 30 mA. A preliminary set of cell constants and an orientation matrix were calculated from total 36 frames. The optimized strategy used for data collection consisted different sets of φ and ω scans with 0.5° steps in φ/ω . Data were collected keeping the sample-to-detector distance fixed at 5.00 cm. The X-ray data acquisition was monitored by APEX2 program suit. All the data were corrected for Lorentz-polarization and absorption effects (Multi scan) using SAINT and SADABS programs integrated in APEX2 package.¹ The structures were solved by direct methods and refined by full matrix least squares, based on F^2 , using SHELX-97.² Molecular diagrams were generated using ORTEP-3³ and Mercury programs.⁴ Geometrical calculations were performed using SHELXTL² and PLATON.⁵ The H atoms in **1** (phenyl), **2** (pyrrolidine) and **5** (piperidine) crystals were placed in idealized positions (C-H = 0.93 Å for the phenyl H atoms, C-H = 0.97 Å for the methyl H-atoms and N-H=0.86 Å for the amide H atom) and constrained to ride on their parent atoms [$U_{\text{iso}}(\text{H}) = 1.2 U_{\text{eq}}(\text{C})$]. The H-atoms for the **3** (dimethyl), **4** (morpholine) and **6** (pyridine) crystals were also placed in idealized positions however with different C-H distances (C-H = 0.95 Å for the phenyl H atoms, C-H = 0.99 Å for the methyl H-atoms and N-H=0.88 Å for the amide H atom) and constrained to ride on their parent atoms [$U_{\text{iso}}(\text{H}) = 1.2 U_{\text{eq}}(\text{C})$]. The crystals of **6** (pyridine) showed the presence of disordered molecule of unknown solvent.

Table S1: Crystallographic data table for compounds **1-6**

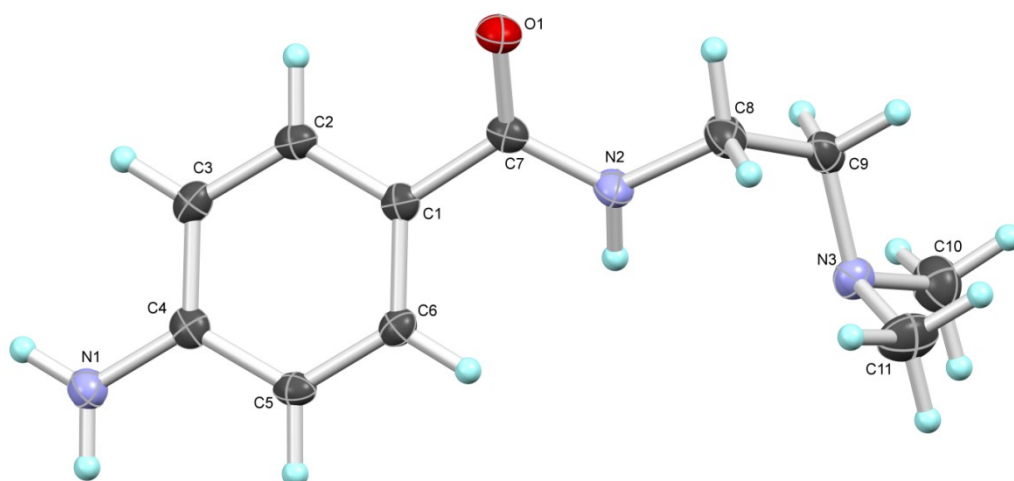
Crystal Data	1(Phenyl)	2(Pyrrolidine)	3(Dimethyl)	4(Morpholine)	5(Piperidine)	6(Pyridine)
Formula	C ₁₅ H ₁₆ N ₂ O	C ₁₃ H ₁₉ N ₃ O	C ₁₁ H ₁₇ N ₃ O	C ₁₃ H ₁₉ N ₃ O ₂	C ₁₄ H ₂₁ N ₃ O	C ₁₄ H ₁₅ N ₃ O
M _r	240.30	233.31	207.28	249.31	247.34	241.29
Crystal Size, mm	0.25 x 0.09 x 0.06	0.09 x 0.08 x 0.03	0.28 x 0.12 x 0.08	0.32 x 0.12 x 0.09	0.25 x 0.09 x 0.07	0.15 x 0.08 x 0.05
Temp. (K)	296(2)	296(2)	100(2)	100(2)	296(2)	296 (2)
Crystal Syst.	Orthorhombic	Orthorhombic	Orthorhombic	Orthorhombic	Orthorhombic	Tetragonal
Space Group	<i>P</i> 2 ₁ 2 ₁ 2 ₁	<i>P</i> 2 ₁ 2 ₁ 2 ₁	<i>P</i> 2 ₁ 2 ₁ 2 ₁	<i>P</i> 2 ₁ 2 ₁ 2 ₁	<i>P</i> 2 ₁ 2 ₁ 2 ₁	<i>P</i> -4 2 ₁ c
<i>a</i> /Å	9.5732(13)	6.391(3)	5.9755(3)	9.3267(14)	9.624(2)	19.628(6)
<i>b</i> /Å	9.6932(13)	13.847(7)	13.1272(8)	9.8628(15)	10.246(3)	19.628(6)
<i>c</i> /Å	14.0706(18)	14.418(7)	14.4992(8)	14.061(2)	13.768(3)	8.151(3)
α°	90	90	90	90	90	90
β°	90	90	90	90	90	90
γ°	90	90	90	90	90	90
<i>V</i> /Å ³	1305.7(3)	1276.0(11)	1137.34(11)	1293.4(3)	1357.5(6)	3140.0(17)
Z	4	4	4	4	4	8
<i>D</i> _{calc} /g cm ⁻³	1.222	1.214	1.211	1.280	1.210	1.173
<i>m</i> /mm ⁻¹	0.078	0.079	0.080	0.088	0.078	0.075
<i>F</i> (000)	512	504	448	536	536	1168
<i>Ab. Correct.</i>	multi-scan	multi-scan	multi-scan	multi-scan	multi-scan	multi-scan
<i>T</i> _{min} / <i>T</i> _{max}	0.9953/ 0.9808	0.9980/0.9929	0.9936/ 0.9779	0.9921/ 0.9723	0.9945/ 0.9807	0.9880 / 0.9977
2 θ _{max}	50	50	50	50	50	50
Total reflns.	13719	6182	5135	6521	5609	36254
unique reflns.	2289	2235	1995	2263	2383	1722
<i>h, k, l</i> (min, max)	(-11, 10), (-11, 11), (-15, 16)	(-7, 7), (-16, 14), (-17, 16)	(-7, 6), (-15, 11), (-17, 14)	(-11, 11), (-11, 11), (-16, 13)	(-11, 11), (-5, 12), (-16, 16)	(-23, 23), (-19, 23), (-9, 9)
R _{int}	0.0645	0.0566	0.0275	0.0229	0.0766	0.1064
No. of para	163	163	139	163	164	190
<i>R</i> 1 [<i>I</i> > 2 σ (<i>I</i>)]	0.0671	0.0567	0.0306	0.0305	0.0643	0.0775
<i>wR</i> 2 [<i>I</i> > 2 σ (<i>I</i>)]	0.1611	0.1347	0.0812	0.0757	0.1486	0.1824
<i>R</i> 1 [all data]	0.0885	0.1058	0.0319	0.0322	0.0790	0.1354
<i>wR</i> 2 [all data]	0.1711	0.1635	0.0824	0.0766	0.1626	0.2077
goodness-of-fit	1.236	0.998	1.045	1.089	1.004	1.050
$\Delta\rho_{\max}, \Delta\rho_{\min}$ (eÅ ⁻³)	+0.331, -0.249	+0.177, -0.147	+0.249, -0.211	+0.235, - 0.173	+0.359, -0.333	+ 0.477, - 0.252
CCDC no.	1425934	1425935	1425936	1425937	1425938	1442290



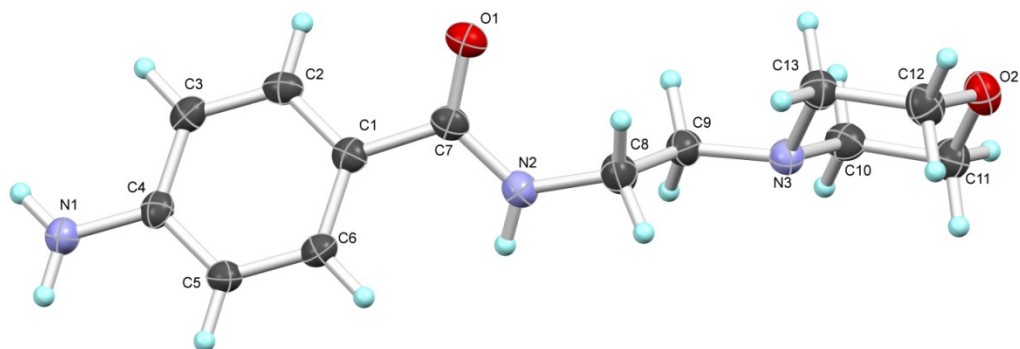
(a)



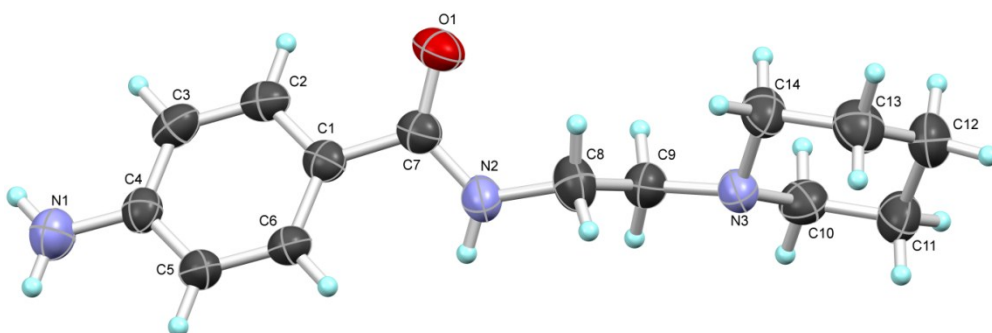
(b)



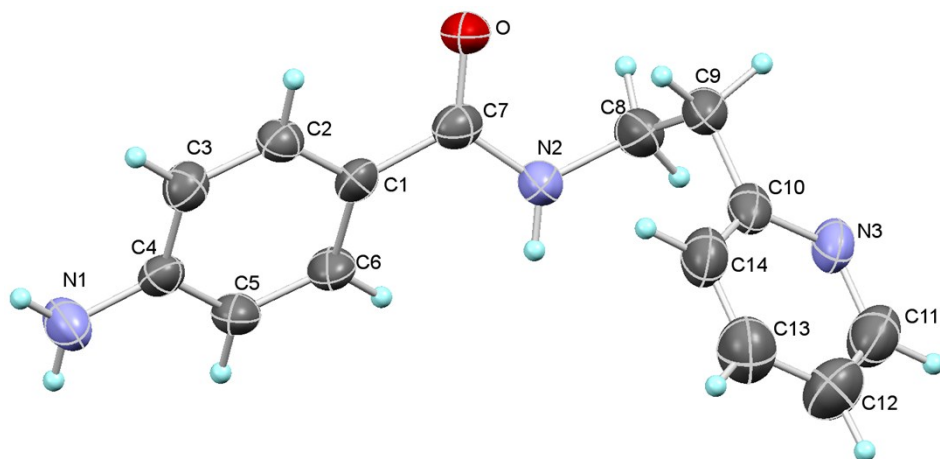
(c)



(d)



(e)



(f)

Figure S20. ORTEPs of compound (a) **1** (b) **2** (c) **3** (d) **4** (e) **5** and (f) **6**. For clarity the disordered atoms in the crystal of **2** (pyrrolidine) and disordered solvent molecule in the crystal of **6** (pyridine) were not shown.

Differential Pulse Voltammetry

(DPV) was performed using CHI 900b potentiostat with pulse amplitude of 50 mV, pulse width of 0.2 s and a pulse period of 0.5 s. A three electrode system containing glassy carbon (GC, 3 mm diameter) as working electrode, Pt-foil as counter electrode and a standard calomel electrode (SCE, 0.1 M KCl) as reference electrode, was employed for this purpose. 0.1 M phosphate buffer (pH 7.4) was used as electrolyte. 0.1 M stocks were prepared for Procainamide, compounds **1-6** and 2-deoxyguanosine (dG) in cell culture grade DMSO. The solutions of dG and compound were mixed thoroughly and the dG to compound ratio was kept constant at 4.0 for all the experiments. All the solutions were incubated at 37°C for 1 h before doing DPV experiments. Final concentrations of dG and compounds were 790.5 μM and 197.6 μM respectively. Potential was scanned from anodically from -0.25 to 1 V vs SCE with an increment in potential of 4 mV at 30°C. Each measurement was repeated thrice and the average was taken as the final result. The surface of GC electrode was renewed every time by mechanical polishing with 0.1 μm alumina powder followed by sonication in deionized (DI) water for 5 min. Similarly, the electrochemical cell was also washed thoroughly after each experiment.

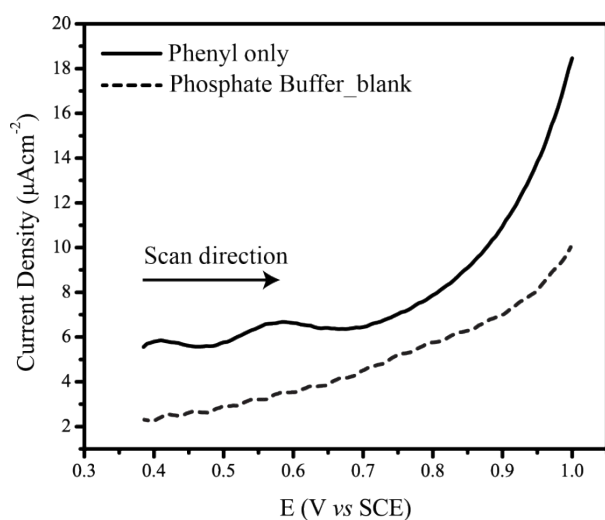


Figure S21. Differential pulse voltammogram of phenyl derivative **1** alone under identical condition used for the study of compound-dG interactions, DPV for only buffer (blank) is also shown for comparison; appearance of peak in case of phenyl drug suggests its oxidation.

Docking Study:

To perform the molecular docking, starting conformations of compound **1-6** were extracted from their crystal coordinates. Bioactive conformations were generated using MacroModel module and further minimized with OPLS2005 force field in Maestro 9.1 (Schrödinger LLC, New York, NY, 2010). Generated possible conformations of compounds were further used for docking study. Crystal structures of CpG rich partially denatured hemimethylated (hmDNA) were obtained from the PDB ID: 4DA4. Protein preparation wizard was utilized to remove protein component and perform optimization. DNA biomolecule was subjected to restrained minimization using OPLS 2005 force-field. Further grids were generated so that entire DNA molecules fit within grid box and the centre lies at the centroid of DNA strands. The larger gridbox size was used to allow docking with entire DNA molecule. Flexible docking method was performed with extra-precision (XP) implemented in Glide without applying constraints during docking. The post docking minimization was performed and binding energy with interacting residues was calculated. Docking poses were filtered based cut-off assigned for τ_1 which is 160° - 180° . Torsion angle parameters and structure overlay of ligand conformations from chosen docked poses are depicted in figure S23 and table S3.

Glide Score	H-bond Score(E1)	Van der Waals Energy score (E2)
It is an empirical scoring function that estimates the ligand bonding free energy. It is inclusive of (electrostatic, van der Waals) contributions as well as rewarding or penalizing interactions which influence ligand binding. It is used to score docked poses and compare their relative binding affinities. ⁶	The H-bond per-residue interaction term is calculated for estimating the strength of H-bonding interaction between the ligand and a given residue. The more negative score suggests stronger hydrogen bonding. The score takes into account the types of atoms involved and geometry of hydrogen bonding. ⁷	Van der Waals energy term (E2) gives the estimates van der Waals association and steric attraction between ligand and given residue. ⁸

CSD survey

CSD survey was carried out using CCDC conquest version 1.17.⁹ The molecular structure of the query is depicted in figure below. Torsion angle τ_1 (C1-C7-N2-C8) was used as parameter for statistical analysis. Almost for 92 % hits torsion angle τ_1 lies within the range of 160.112° - 179.980° .

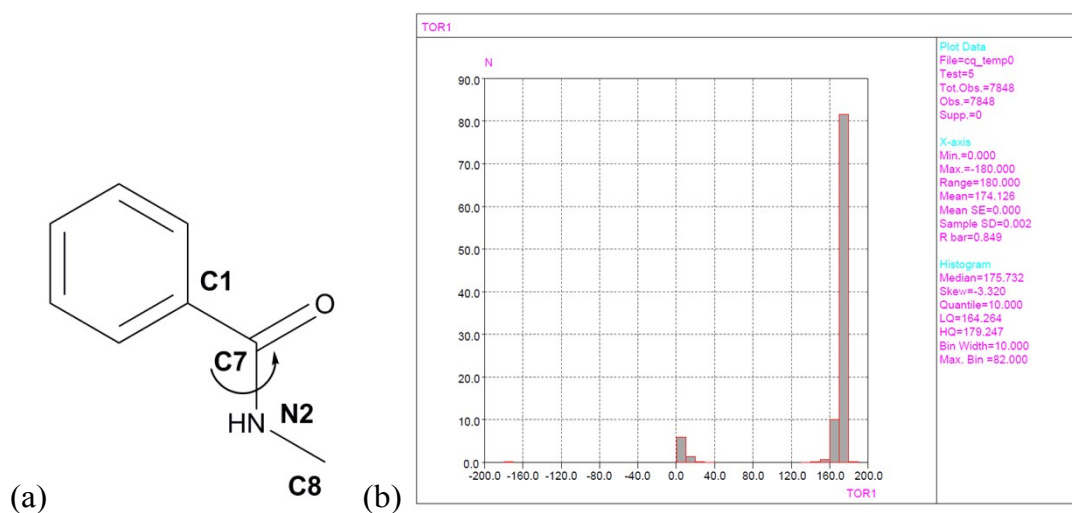


Figure S22. (a) Molecular structure of query Compound (b) XY plot of X-torsion range and Y- number of hits in %

Table S2. Number of hits, torsion angle range and % hits

No of hits	Range (°)	%
6398	170.002-179.980	81.92
785	160.112-169.994	10.05
54	150.098-159.950	0.691
463	0-9.926	5.92
110	10.012-19.667	1.40

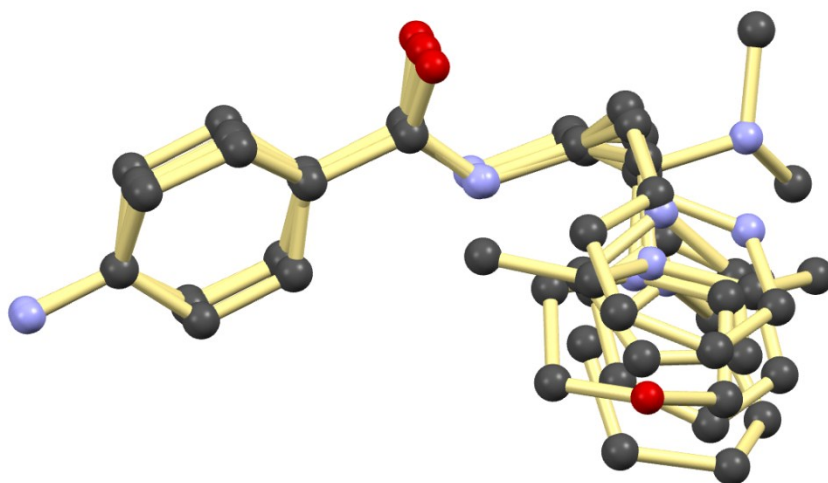


Figure S23. Overlay of ligand conformations of compounds **1-6** and Procainamide extracted from docked poses.

Table S3. Torsion angle table τ_1 of ligand conformations from selected docked poses.

Compounds	Phenyl	pyrrolidine	piperidine	Morpholine	dimethyl	pyridine	Procainamide
Torsion τ_1	179.22	-178.84	-178.81	-175.69	178.58	177.75	179.45

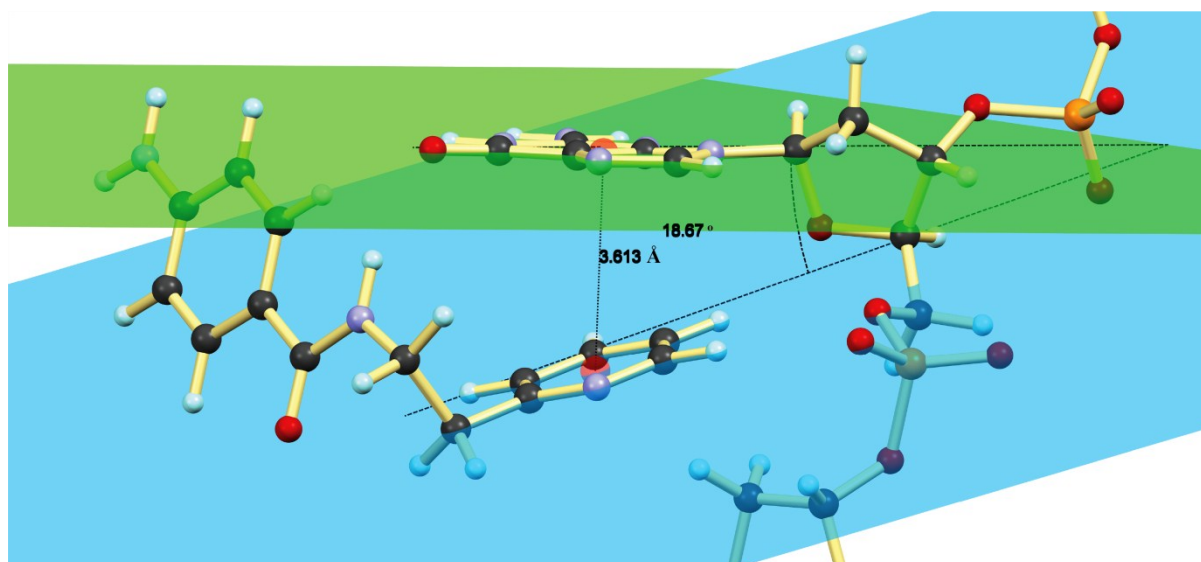


Figure S24. $\pi \cdots \pi$ stacking geometry of compound **6 (pyridine)** with dG base at the target site (extracted from docked pose) displaying Cg \cdots Cg distance (centroid to centroid distance between aromatic rings) and dihedral angle α between the aromatic rings.

Cytotoxicity Assay:

The cell lines MCF-7 were procured from National Center for Cell Sciences Repository, Pune. Cell viability after compound treatment was analyzed by MTT assay. MCF-7 cells were seeded in 96-well plate (day 0) with seeding density of ~7500 cells/well. After 24h, the media was changed and 5µl of compound dissolved in DMSO at concentration ranging from 500µM to 100µM was added to 95µl media (final DMSO conc. 0.5%). Control wells contained cells in MEM media or cell treated with 0.5% DMSO (DMSO control). The plates were incubated at 37°C in 5% CO₂ incubator overnight. After 24 h., 10µl of 3-(4,5-dimethylthiazol-2-yl)-2,5-diphenyltetrazoliumbromide (MTT, Himedia, 0.5mg/ml) was added in culture medium in each well. After 3.5 h incubation at 37°C in 5% CO₂, the culture media was removed and 150µl of DMSO (HiMedia, India) was added in each well to dissolve the formazan salts. The absorbance of the color developed was recorded at 550nm and 620nm using Automatic plate reader. The independent experiments were set up in biological triplicates for 24, 48, and 72 hrs. and each experiment was performed in technical and biological triplicates. The graph for cell viability was plotted using Microsoft Excel 2007 version and performed One-way ANOVA to test the statistical significance for the outcomes at $P < 0.05$.

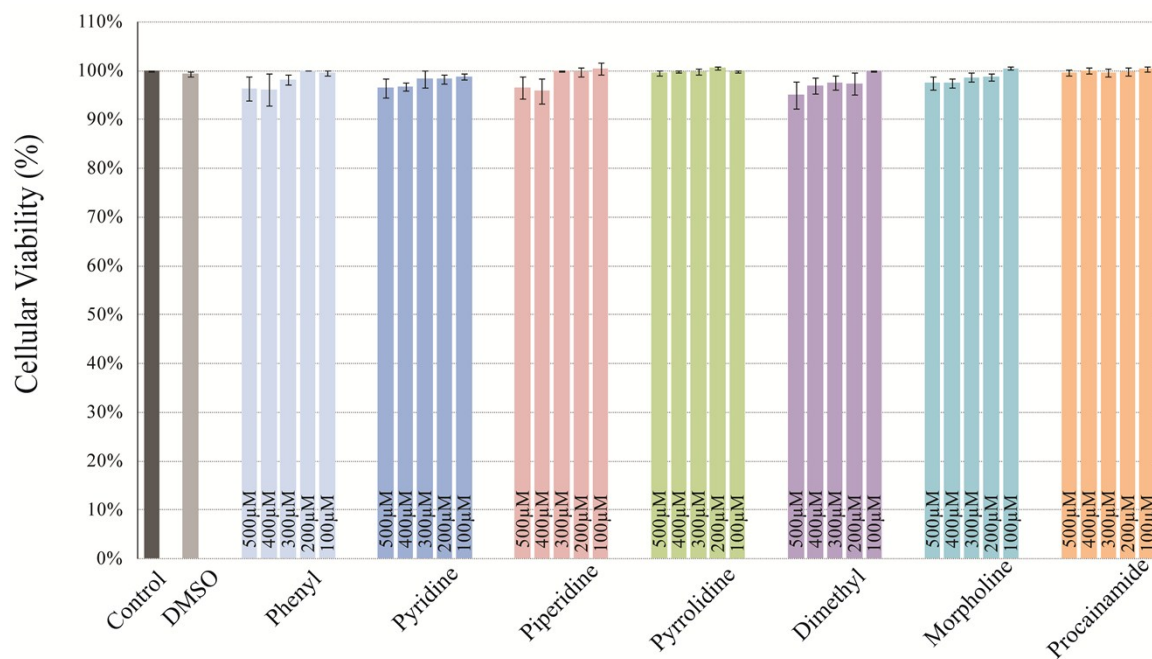


Figure S25. Cell viability study after 24h time point for compounds **1-6** and Procainamide and concentration ranging from 100-500μM. (X axis: conc. of compounds and Y axis: Cell viability in %)

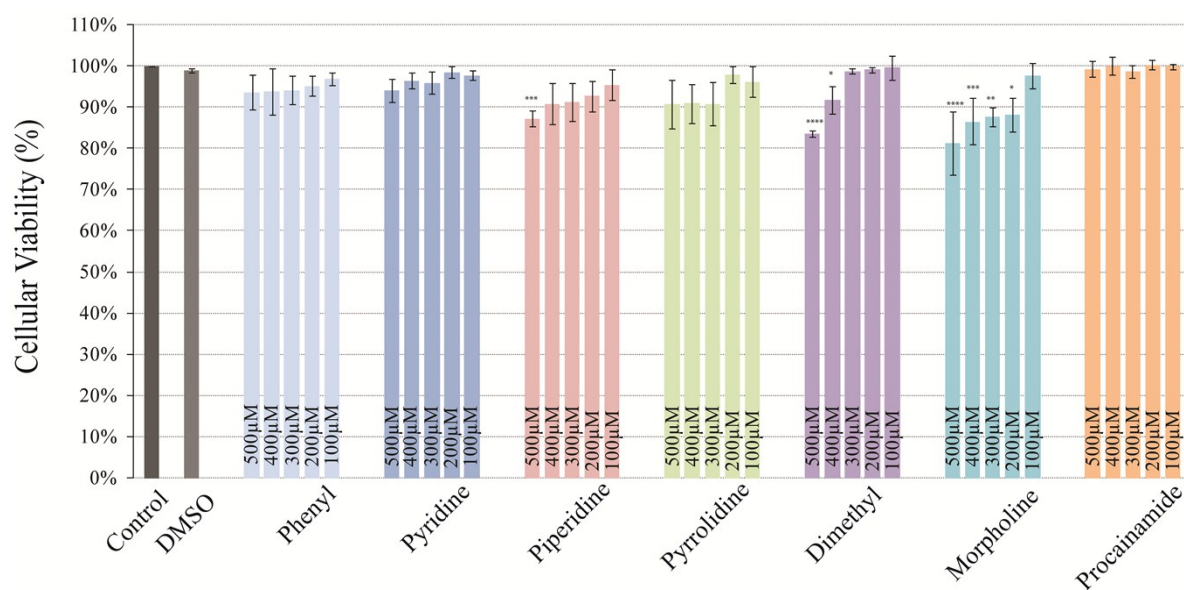


Figure S26. Cell viability study after 48h time point for compounds **1-6** and Procainamide and concentration ranging from 100-500μM. (X axis: conc. of compounds and Y axis: cell viability in %)

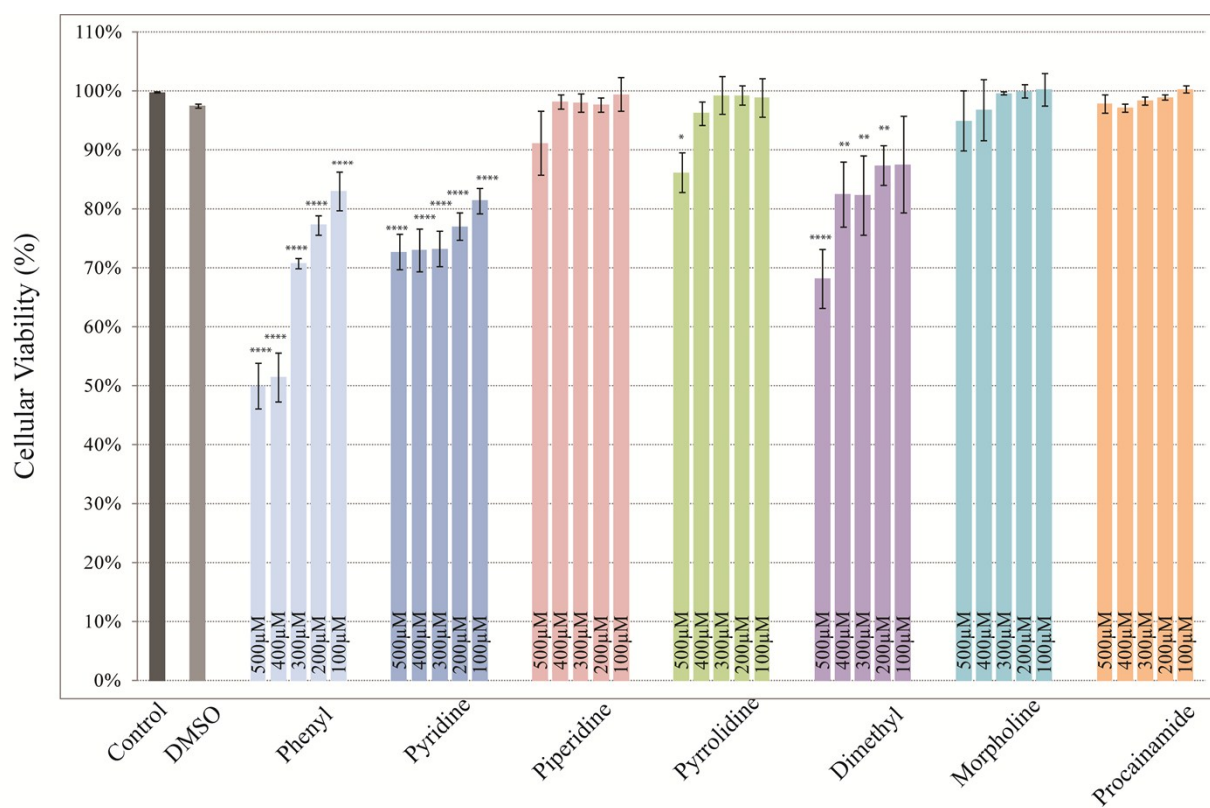


Figure S27. Cell viability study after 72h time point for compounds **1-6** and Procainamide and concentration ranging from 100-500 μM. (X axis: conc. of compounds and Y axis: cell viability in %)

Global methylation quantification assay

The experiment was performed using EpiSeeker methylated DNA Quantification Kit (ab117128) as per the Manufacturer's protocol¹⁰. MCF-7 cells with a density of $\sim 1 \times 10^6$ cells in T-25 flasks were treated with 25 μ l of compounds (100 μ M, 0.5% DMSO) for 72 hrs. at 37°C in 5% CO₂ incubator. After 72 h, DNA was isolated from cells using Phenol: Chloroform method. The purity of the DNA was determined by 260/280 ratio. 100ng of the isolated pure DNA were bound with binder solution to the wells provided by the kit. As such the plate was incubated at 37°C for 90min. The DNA was washed with buffer to remove excess of binding solution. It was then incubated with primary antibody for 1 hr. at 37°C, followed by secondary antibody for 30min at RT. The relative percentage of 5-methylCytosine were colorimetrically quantified by reading absorbance at 450nm. The experiments were performed in technical duplicate and biological triplicates. The graphs were plotted using OriginLab software.

Calculation

$$5\text{mC } \% = \left(\frac{(\text{Sample OD} - \text{Negative Control OD}) / \text{Sample DNA (ng)}}{((\text{Positive Control OD} - \text{Negative Control OD}) \times 2) / \text{Positive Control DNA (ng)}} \right) \times 100$$

DNMT-1 inhibition assay

For DNMT1 assay EpiQuik DNA Methyltransferase 1 Activity/Inhibitor Screening Assay Core Kit (P-3006A) has been used and the protocol for the assay is followed as per the manufacturer's instruction¹¹. The compounds (**1** phenyl and Procainamide) at 100 μ M conc. (DMSO at 0.01%) are incubated with substrate and pure DNMT1 protein for 1.5 hrs in assay buffer. As control experiment DMSO at 0.01% also have been tested but not included in the graph due to obvious minute level of inhibition. The inhibition is then colorimetrically quantified using antibody specific for 5-methylCytosine and reading absorbance at 450nm. The result is expressed in percent inhibition using the given formula. The experiments were performed in triplicates.

$$\text{Inhibition \%} = 1 - \frac{\text{OD (no inhibitor control - blank)}}{\text{OD (inhibitor sample - blank)}} \times 100\%$$

References

- (1) Bruker, 2007; APEX2, SAINT, and SADABS: Bruker AXS Inc., Madison, Wisconsin, USA.
- (2) Sheldrick, G. M. *Acta Cryst.* 2008, *A64*, 112 – 122.
- (3) Farrugia, L. J. *J. Appl. Cryst.* 2012, *45*, 849-854.
- (4) Macrae, C. F.; Bruno, I. J.; Chisholm, J. A.; Edgington, P. R.; McCabe, P.; Pidcock, E.; RodriguezMonge, L.; Taylor, R.; van de Streek, J.; Wood, P. A. *J. Appl. Crystallogr.* 2008, *41*, 466-470.
- (5) Spek, A. L. *Acta Cryst.* 2009, *D65*, 148-155.
- (6) <http://www.schrodinger.com/kb/1027>
- (7) <http://www.schrodinger.com/kb/635>
- (8) <http://www.schrodinger.com/kb/731>
- (9) I. J. Bruno, J. C. Cole, P. R. Edgington, M. Kessler, C. F. Macrae, P. McCabe, J. Pearson and R. Taylor, *Acta Cryst.*, 2002, *B58*, 389-397.
- (10) C. S. Panikar, S. N. Rajpathak, V. Abhyankar, S. Deshmukh, D. D. Deobagkar, *Molecular Biology Reports*, 2015, *42*(12), 1615-21.
- (11) R. Zhang, K.A. Kang, K.C. Kim, S.Y. Na, W.Y. Chang, G.Y. Kim, H.S. Kim, J.W. Hyun, *Gene*, 2013, *524*(2), 214-9.